Materials Science and Engineering A 533 (2012) 64–70

Contents lists available at SciVerse ScienceDirect

Materials Science and Engineering A

journal homepage: www.elsevier.com/locate/msea

Effect of cooling rate during solidification of Sn–9Zn lead-free solder alloy on its microstructure, tensile strength and ductile–brittle transition temperature

K.N. Prabhu*, Parashuram Deshapande, Satyanarayan

Department of Metallurgical & Materials Engineering, National Institute of Technology Karnataka, Surathkal, Mangalore 575 025, India

ARTICLE INFO

Article history:
Received 7 October 2011
Received in revised form
14 November 2011
Accepted 15 November 2011
Available online 23 November 2011

Keywords:
Lead-free solder
Cooling rate
Solidification
Microstructure
UTS
DBTT

ABSTRACT

Solidification rate is an important variable during processing of materials, including soldering, involving solidification. The rate of solidification controls the metallurgical microstructure at the solder joint and hence the mechanical properties. A high tensile strength and a lower ductile–brittle transition temperature are necessary for reliability of solder joints in electronic circuits. Hence in the present work, the effect of cooling rate during solidification on microstructure, impact and tensile properties of Sn–9Zn lead-free solder alloy was investigated. Four different cooling media (copper and stainless steel moulds, air and furnace cooling) were used for solidification to achieve different cooling rates. Solder alloy solidified in copper mould exhibited higher cooling rate as compared to other cooling media. The microstructure is refined as the cooling rate was increased from 0.03 to 25 °C/s. With increase in cooling rate it was observed that the size of Zn flakes became finer and distributed uniformly throughout the matrix. Ductile-to-brittle transition temperature (DBTT) of the solder alloy increased with increase in cooling rate. Fractured surfaces of impact test specimens showed cleavage like appearance and river like pattern at very low temperatures and dimple like appearance at higher temperatures. The tensile strength of the solder alloy solidified in Cu and stainless moulds were higher as compared to air and furnace cooled samples. It is therefore suggested that the cooling rate during solidification of the solder alloy should be optimum to maximize the strength and minimize the DBTT.

1. Introduction

Eutectic or near eutectic Sn–Pb solder alloys have been widely used as filler materials in electronic packaging due to their lower melting temperature, better wetting behavior and mechanical properties. However, due to environmental and human health concern use of Pb in electronic applications has been banned since July 1, 2006 in most of the western countries [1]. Thus, lead-free solders are widely used in electronic packaging to replace Sn–37Pb solder. Sn–9Zn lead free solder alloy has attracted considerable attention and is one of the best alternative choices to replace eutectic Sn–Pb solder because of its melting temperature near to that of Sn–37Pb solder (MP = 198 °C) and its lower compared to Ag bearing solders [1–3].

The microstructure, tensile, and creep behavior of bulk Sn–3.5Ag solder were studied as a function of cooling rate by Ochoa et al. [4,5]. The secondary dendrite arm size and spacing of the tin-rich phase, as well as the morphology of Ag_3Sn were affected by the cooling rate. Both the yield strength in tension and creep resistance of the alloy increased with increasing cooling rate while the strain-to-failure decreased. Solidification rate of the solder joint depends on how fast a heat source is removed from the joint, the size of the joint and on the materials surrounding the joint [6]. A slower solder solidification process creates finer grains and whereas rapid cooling creates finer grains. The microstructure and shear strength characteristics of pure Sn and the eutectic compositions of Sn–37Pb, Sn–0.7Cu, and Sn–3.5Ag prepared under identical reflow conditions but subjected to two different cooling conditions were evaluated at room temperature by Maveety et al. [7]. Decreasing the cooling rate tended to decrease the ultimate shear strength of solder alloys.

An investigation on the effects of cooling rate on the microstructure and tensile behavior of a Sn–3.5 wt.%Ag Solder revealed the significant effect of the cooling rate on mechanical behavior of the solder. Yield strength was found to increase with increasing cooling rate, although ultimate tensile strength and strain-to-failure seemed unaffected by the cooling rate [8]. The influence of cooling rate on the creep behavior of Sn–9%Zn and Sn–8%Zn–3%Bi solder alloys was studied by impression testing. The alloys were prepared at two different cooling rates of 0.01 K s^{-1} and 8 K s^{-1}. This affected the microstructure and thus, the creep behavior of the materials [9]. An investigation of the microstructure and microhardness of Sn–Cu and Sn–Ag solders as functions of alloy composition and cooling rate was carried out by Seo et.al. [10]. It was found that both alloy

* Corresponding author. Fax: +91 8242474033.
E-mail address: prabhukn_2002@yahoo.co.in (K.N. Prabhu).

0921-5093/$ – see front matter © 2011 Elsevier B.V. All rights reserved.
doi:10.1016/j.msea.2011.11.035

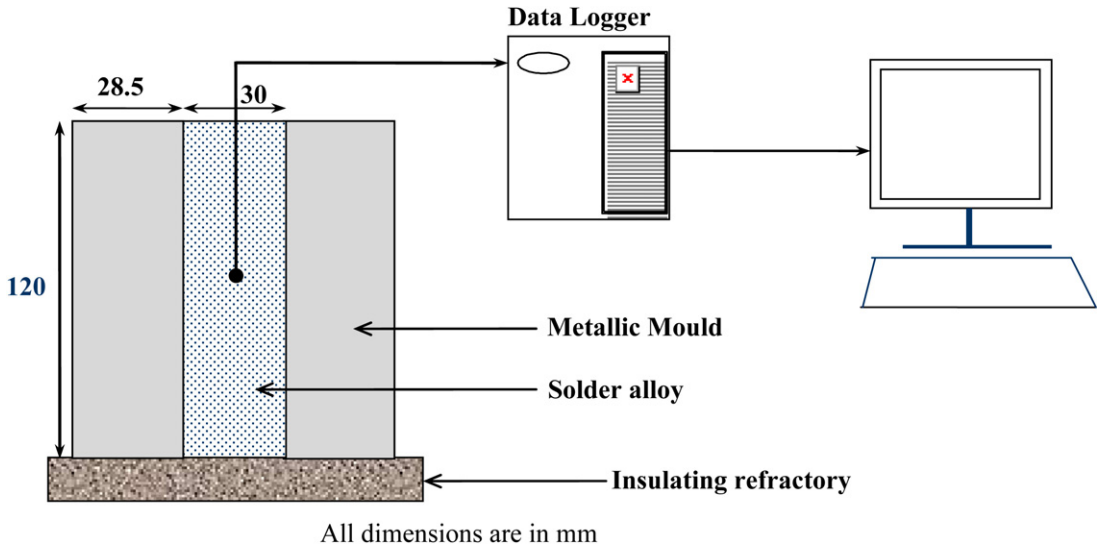

Fig. 1. Schematic sketch of experimental set up for solidification in moulds.

composition and cooling rate can significantly affect the Sn grain size and hardness in Sn-rich solders. The literature review thus suggests that the mechanical properties of the soldering joints are significantly affected by the solidification/cooling rate of the solder because the microstructures of solder joints are strongly dependent on these parameters.

It is well known that, some materials including solder alloys exhibit a transition from ductile-to-brittle behavior when tested above and below a certain temperature called the 'Ductile-to-brittle transition temperature' (DBTT). Below this transition temperature many solder materials exhibit brittle fracture. The ductile-to-brittle temperature is therefore an important parameter to be considered while selecting a lead free solder. Generally, lead-free solders are stiffer, deform less easily than lead base solders and with increase in the level of locally accommodated stresses the probability of crack nucleation increases [11,12]. Eventually the crack propagation leads to major failure of solder joint.

The rate of solidification controls the metallurgical microstructure at the solder joint and hence the mechanical properties. A high tensile strength and a lower ductile–brittle transition temperature are needed for better reliability of solder joints in components involving electronic circuits. Among lead free solders Sn–9Zn alloy is cheap compared to silver bearing solders. The objective of the present work is to study the effect of cooling rate during solidification on microstructure, tensile strength and impact properties of Sn–9Zn lead-free solder alloy.

2. Experimental

Sn–9Zn alloy was prepared using commercially procured ingots of pure Sn and Zn alloys with 99.9+% purity. The ingots were mixed in right proportions and melted in an electric resistance furnace to produce Sn–9Zn solder ingots. Cast ingots of the Sn–9Zn alloy were re-melted and solidified in copper and stainless steel moulds as well as in crucible open to atmosphere (air) and in furnace to achieve different cooling rates during solidification. The casting temperature was 240 °C. The moulds used were of dimensions 30 mm inner diameter and 120 mm height and thickness 28.5 mm. A calibrated twin bore ceramic beaded 1 mm K-type thermocouple was placed at the geometric centre of the mould/crucible to monitor the thermal history of the solidified melt (Fig. 1). The thermocouple was connected to a high speed online data acquisition system NI SCXI 1000 to measure the cooling rate of the solidifying solder alloy. Temperature data was acquired at a rate of 60 samples per second in these experiments.

Charpy V-notch (CVN) and tensile specimens were made from sections, where the cooling rate was measured. The test specimens used were rectangular bars of dimensions 10 mm × 10 mm × 55 mm with V-notch 1.5 mm for Charpy test (ASTM E23 standard) and 36 mm in gauge length, 9 mm in diameter, radius of fillet 8 mm and length of reduced section is 45 mm for tensile specimen (ASTM E8). A pendulum impact tester (JM Tools, New Delhi) and Hounsfield Tensometer (Tensometer Ltd., England) were used to measure the impact and tensile properties of the solder alloy. Before finding the properties of the solder alloy, machined specimens were annealed at 130 °C for 15 min to relieve the residual stresses generated during machining of solder alloy. CVN solder specimens were tested in impact between −100 °C and 30 °C to investigate the temperature dependence of solder fracture behavior. Cooling of test specimens was done in dry ice or with the aid of ethanol cooled with liquid nitrogen. The energy absorbed for each sample tested at different temperatures was directly read from the Charpy V-notch impact tester. DBTT of solder was calculated by plotting the graph of energy absorbed vs temperature. Experiments were repeated twice to check the repeatability.

Ultimate tensile strength of solder alloy was calculated from the stress–strain curve. The solder solidified under different cooling media was micro-examined using Zeiss Axio-imager optical microscope. The fractured surfaces were examined using Jeol JSM 6380LA scanning electron microscope (SEM).

3. Results and discussion

The measured values of cooling rates of Sn–9Zn solder solidified in different cooling media (Cu, stainless steel, open to atmosphere and furnace cooling) are tabulated in Table 1. Cooling rate increases with cooling media in the order copper > stainless steel > air cooling >furnace cooling. Solder solidified in copper exhibited higher cooling rate of 24.77 °C/s and furnace cooling showed the lowest (0.03 °C/s).

The cooling rate of solder alloy significantly affected the microstructure of the solder alloy. Fig. 2a–d shows the microstructure of the solder alloy solidified in different cooling media. Microstructure of furnace cooled sample showed both fine as well as coarser needle like Zn rich phase which are dispersed in Sn matrix as shown in Fig. 2a. However zinc flakes were not distributed

Table 1
Cooling rates of Sn–9Zn alloy solidified in different cooling media.

Cooling medium ⟶	Furnace cooled	Air cooled	Stainless steel mould	Copper mould
Cooling rate (°C/s)	0.03	0.31	10	24.77

uniformly. Coarser zinc flakes are formed due to slower cooling rate of the solder alloy that enabled much time for the growth of zinc phases. Microstructure of air cooled showed similar behavior that of furnace crucible cooled. However the zinc flakes were comparatively finer (Fig. 2b). Solder alloy solidified in stainless steel mould and copper mould showed uniformly distributed finer zinc flakes throughout the Sn matrix (Fig. 2c and d). However zinc flakes in solder solidified in stainless steel mould were little coarser compared to Cu mould. Kim et al. [13] also reported that faster cooling of the solder alloy exhibits a much finer and uniform microstructure within which a needle-like Zn phase dispersed in β-Sn matrix is observed. Eutectic Sn–Zn alloy consists of two phases Zn rich phase and β-Sn matrix. Chen et al. [14] reported that during solidification of solder alloy the rod like Zn-rich phases form because of the conglomeration of small Zn rich phase.

The energy absorbed (impact energy) as a function of the test temperatures for Sn–9Zn solder alloy solidified in different cooling media are shown in Fig. 3a–d. It was found that as the cooling rate increases there is increase in DBTT. The values of transition temperature (DBTT) for CVN solder specimens prepared under different solidification media are given in Table 2. It was found that the energy absorbed by the solder specimen increases with increase in temperature just before the transition temperature and it decreases slightly thereafter remaining constant with further increase in temperature. The results showed in Fig. 3 indicate that the solder changes its fracture mode from brittle-to-ductile as the temperature increases. At the point of transition temperature, a drastic change in the impact energy occurs. It is a clear indication of a change in the fracture mode from ductile-to-brittle. Table 2 gives the DBTT values for the various test samples and the data is most essential for electronic applications.

The fractured surfaces of furnace cooled specimens tested under different temperatures are shown in Fig. 4. The solder exhibited river like patterns at lower temperatures (Fig. 4a and b) and dimple like structure at 0 °C. DBTT temperature for solder solidified in furnace was found to be −20 °C. It may be due to coarser zinc flakes offering more resistance to impact. Coarser zinc flakes act as obstacles for dislocation motion during plastic deformation. This is attributed to the accumulation of dislocation pile up near the region of Zn flakes leading to the formation of voids. These voids might act as sites for nucleation of cracks and initiate crack propagation. With increase in cooling rate more zinc needles nucleated. This gives rise to higher probability of void formation and more chance for crack nucleation and propagation. As the cooling rate decreases zinc needles coarsen and consequently with less number of zinc needles there is a lower probability of void formation and fracture. Thus, the refinement of the zinc flakes through solidification process increases DBTT. Ratchev et al. [12] also reported that a lower cooling rate is beneficial to produce coarser precipitate microstructures to decrease the probability of brittle mode

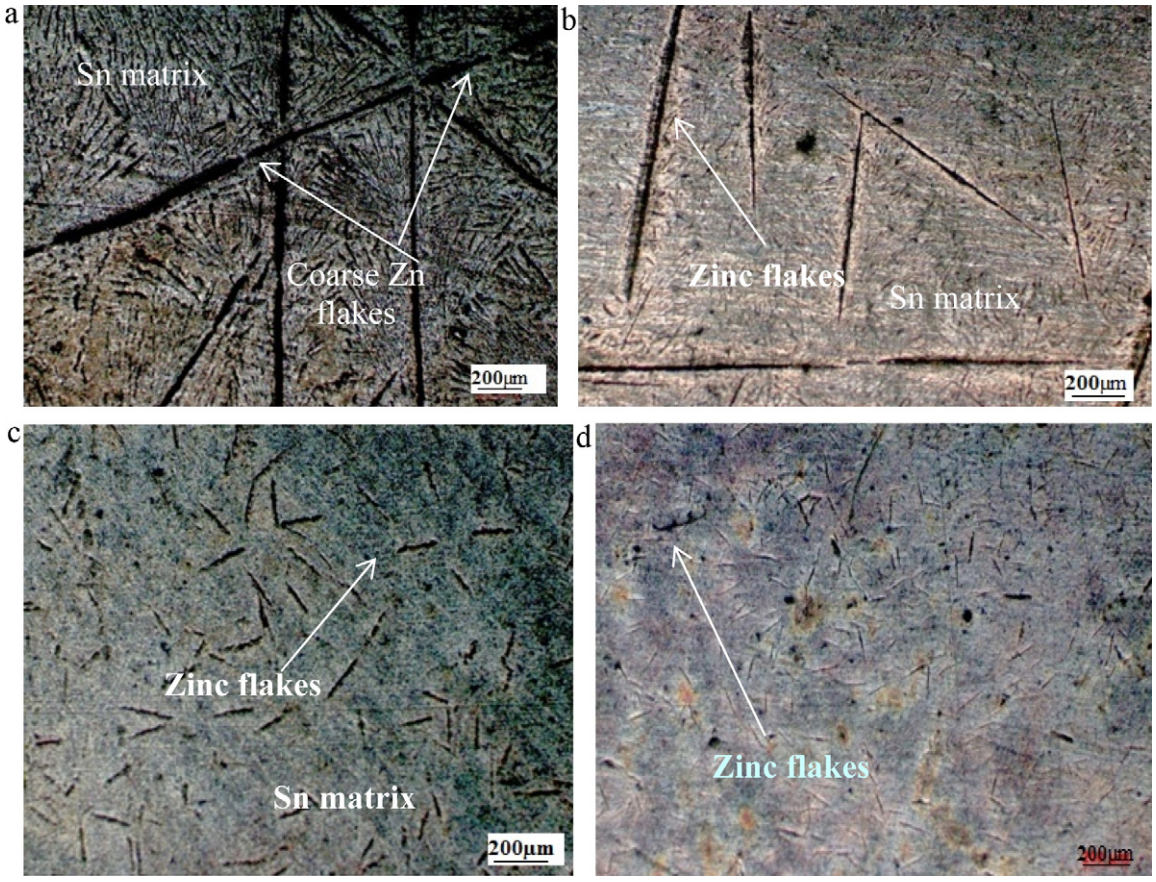

Fig. 2. Microstructure of Sn–9Zn solidified in (a) furnace (b) air (c) stainless steel mould (d) copper mould.

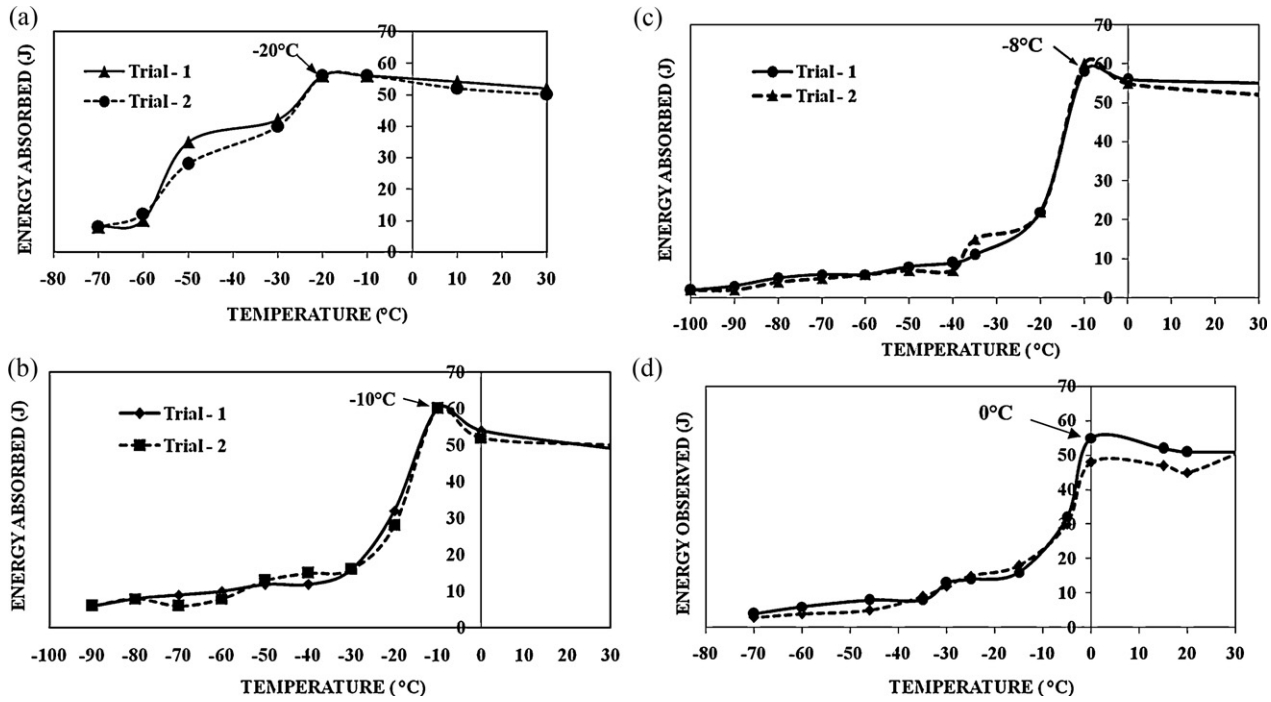

Fig. 3. Impact energy as a function of test temperature for solder solidified in (a) a crucible (furnace cooled) (b) a crucible (air cooled) (c) stainless steel mould and (d) copper mould.

Table 2
Ductile brittle transition temperature (DBTT) of the solder alloy.

Cooling medium ⟶	Furnace cooled	Air cooled	Stainless steel mould	Copper mould
DBTT	−20 °C	−10 °C	−8 °C	0 °C

of failure in solder. Fig. 5 shows the fractured surfaces of solder alloy solidified in air. The fractured surface shows river like pattern which is characteristic feature of brittle fracture. Solder fractured at −40 °C and −20 °C exhibited a mixed mode of fracture i.e. ductile and brittle failure, consisting of both river pattern and dimples as shown in Fig. 5b and c. However, at −20 °C it was found that the fracture was predominantly ductile. Solder fractured at room temperature exhibited stretch marks due to plastic deformation (Fig. 5d) which is a clear indication of ductile failure of the solder alloy.

The fractured surfaces of stainless steel mould cooled specimens tested under different temperatures are shown in Fig. 6. Cleavage fracture was observed for specimen tested at −90 °C and at −50 °C fractured surface showed a mixture of ductile and brittle failure (Fig. 6a and b). This mixed mode completely disappeared at −20 °C showing predominantly ductile failure indicated by the presence of dimples (Fig. 6c). However, at room temperature, fracture did not occur but it showed a plastic deformation. The stretch marks showed in Fig. 6d are due to plastic deformation of the solder. Fig. 7 shows the fractured surfaces of solder alloy solidified in copper mould. Fig. 7a and b clearly shows completely brittle fractured surfaces which are characterized by the stepwise and cleavage like appearance and absence of dimple-rich areas. At −20 °C it shows dimple like structure in some regions as shown in Fig. 7c. At room temperature it clearly showed dimple like appearance (Fig. 7d).

The mechanical properties of solder alloy are found to be strongly dependent on the cooling rate of the solder during solidification. Table 3 gives the measured values of tensile strength of Sn–9Zn solder alloy solidified under different cooling rates. Stress–strain curves of solder alloy obtained under various cooling rates are shown in Fig. 8. Increase in cooling rate significantly increased the ultimate tensile strength of solder alloy. Increase in ultimate strength of solder alloy is obtained with Cu and stainless steel mould cooled samples as compared to air and furnace cooled samples, because finer zinc flakes were distributed uniformly throughout the matrix in Cu and stainless metallic mould

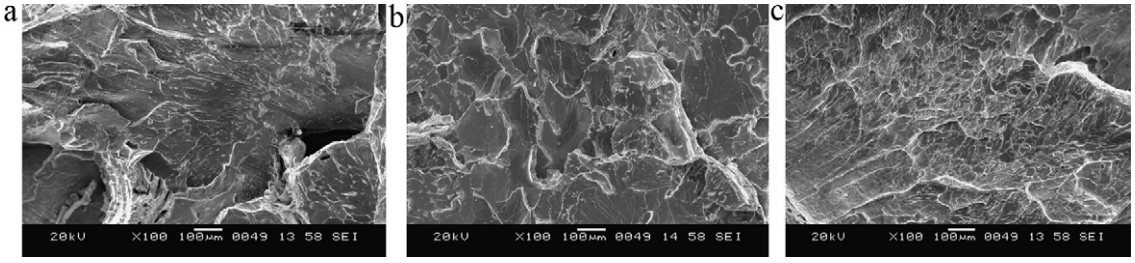

Fig. 4. Fractured surfaces of solder specimen tested in impact at (a) −70 °C (b) −35 °C and (c) 0 °C for furnace cooled samples.

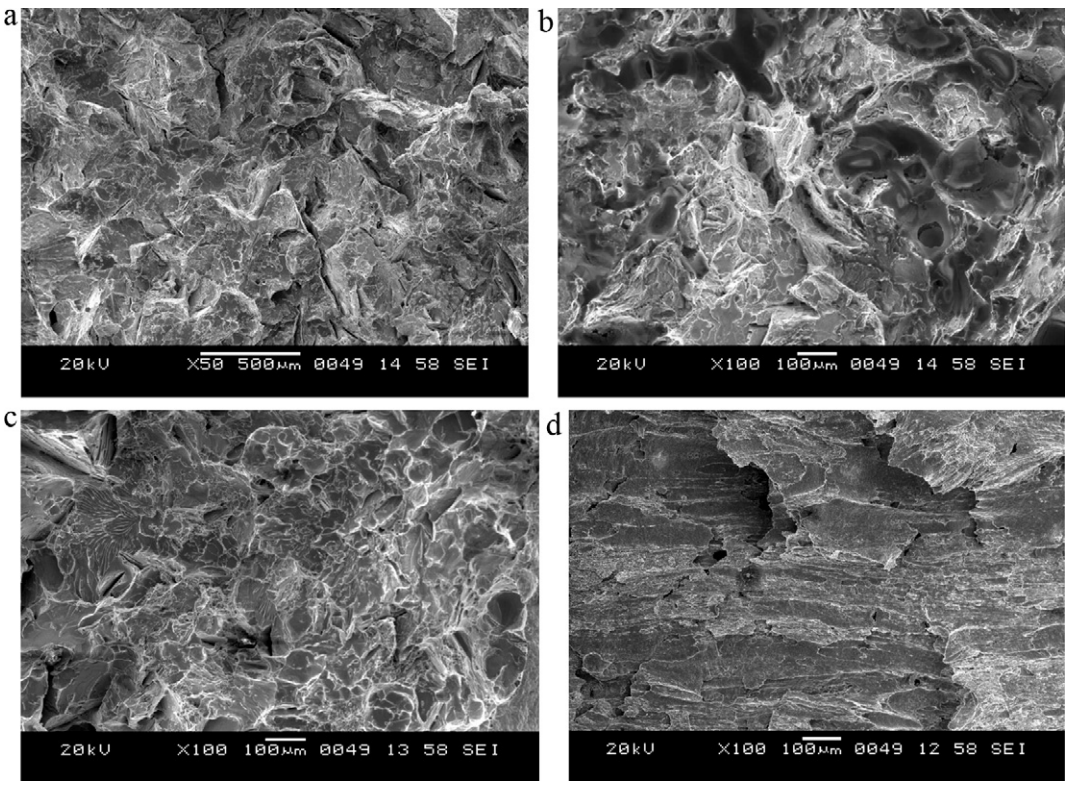

Fig. 5. Fractured surfaces of solder specimen tested in impact at (a) −60 °C (b) −40 °C (c) −20 °C and (d) 30 °C for air cooled samples.

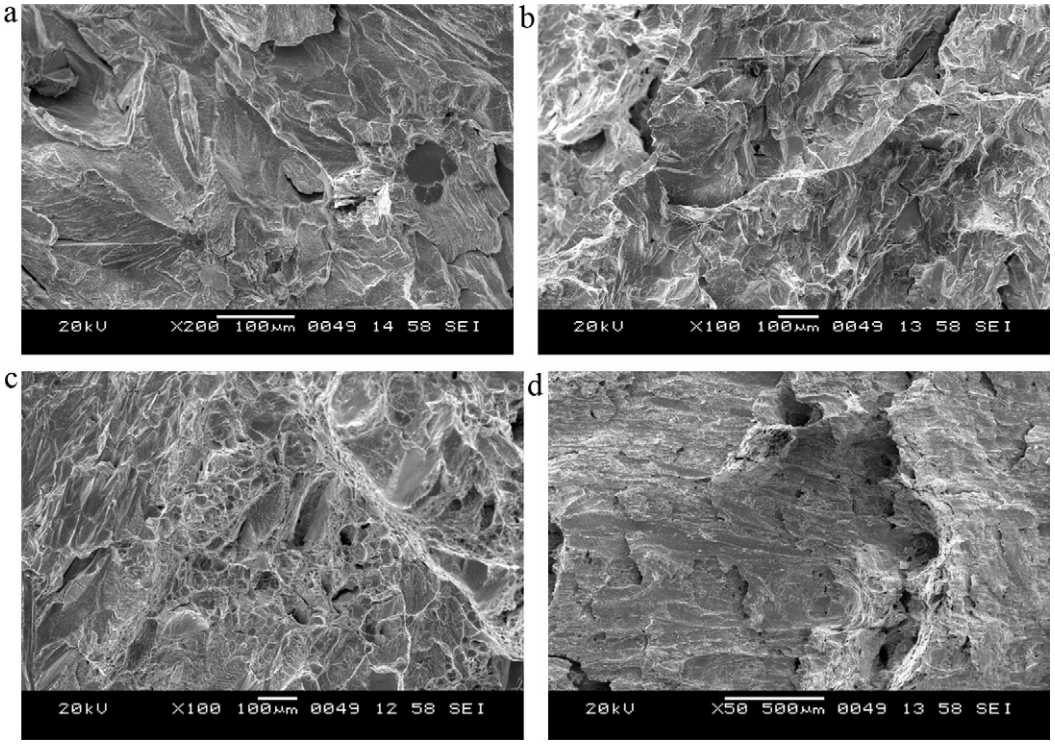

Fig. 6. Fractured surfaces of solder specimen tested in impact at (a) −90 °C (b) −50 °C (c) −20 °C and (d) 30 °C for solder solidified in stainless steel mould samples.

Table 3
Ultimate tensile strength (UTS) of the solder alloy.

Cooling medium ⟶	Furnace cooled	Air cooled	Stainless steel mould	Copper mould
UTS (MPa)	33.6	39.72	44.89	45.02

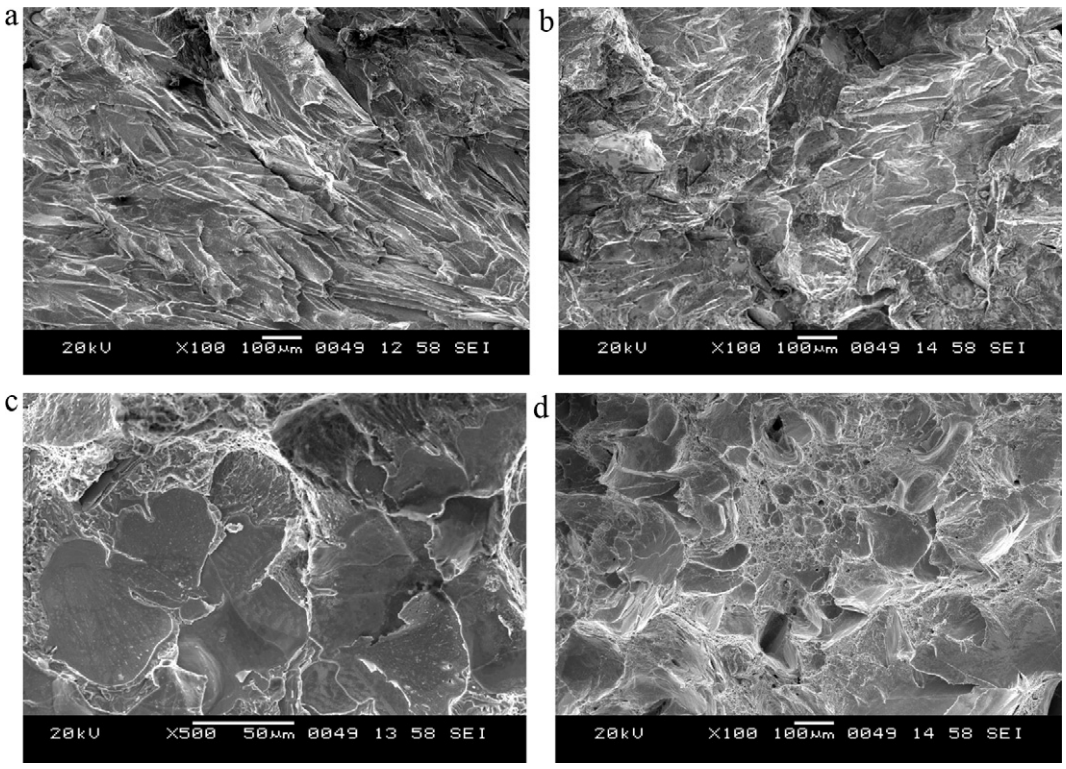

Fig. 7. Fractured surfaces of solder specimen tested in impact at (a) −90 °C (b) −60 °C (c) −20 °C and (d) 30 °C for solder solidified in copper mould samples.

cooled samples (Fig. 2c and d) as compared to specimens prepared in air and furnace (Fig. 2c and d). The strength of air cooled samples decreased due to non uniform distribution of coarser zinc flakes (Fig. 2b). In furnace crucible cooled samples zinc flakes found still coarser and non uniformly distributed in the Sn matrix (Fig. 2a). The coarser Zn flakes in the furnace-cooled samples results in decreased resistance to dislocation motion.

Solder alloy solidified in copper mould with refined Zn rich structures are less resistant to fracture than solder solidified in other systems having a network of precipitated coarser Zn phases in Sn matrix. Further due to the higher strength obtained owing to the faster rate of solidification in copper mould, the ductility of the solder alloy is reduced resulting in a lower impact strength and higher DBTT. The UTS decreased for Sn–9Zn solder alloy solidified at lower cooling rates. However, an increase in cooling rate resulted in the decrease of DBTT of the solder alloy. Hence, the cooing rate of the alloy during solidification of alloy should be controlled for obtaining better reliability of solder joints.

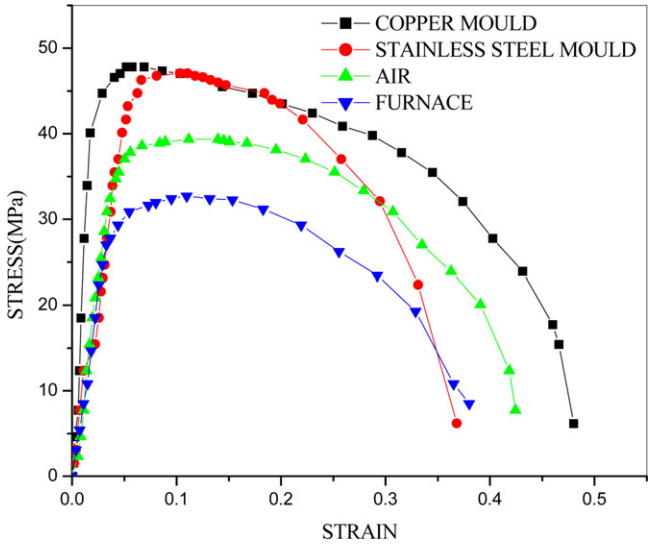

Fig. 8. Stress vs strain curves for the solder alloy solidified at various cooling rates.

4. Conclusions

In the present study the effect of solidification rate on microstructure, impact and tensile properties of Sn–9Zn solder alloy have been investigated. Based on the results and discussion the following conclusions are drawn.

1. Solder alloys solidified in copper mould exhibited higher cooling rates (24.77 °C/s) as compared to stainless steel mould (10 °C/s), air (0.31 °C/s) and furnace (0.03 °C/s) cooled samples.
2. Increase in the cooling rate resulted in finer and uniformly distributed zinc needles throughout Sn matrix.
3. With decrease in cooling rate, DBTT of the solder alloy was found to be lower and this is attributed to the increase in resistance to impact offered by the coarser zinc flakes.
4. DBTT for the solder alloy was found to be −20 °C, −10 °C, −8 °C and 0 °C for furnace and air cooled, stainless steel and copper chilled samples respectively.
5. Solder alloy solidified in Cu and stainless steel mould showed increase in ultimate tensile strength as compared to air and furnace cooled samples. The UTS increased with increase in cooling rate.
6. An optimum cooling rate during solidification is required to yield a solder alloy having higher strength and lower DBTT.

References

[1] R.A. Islam, B.Y. Wu, M.O. Alam, Y.C. Chan, W. Jillek, J. Alloys Compd. 392 (2005) 149–158.

[2] R. Mayappan, A.B. Ismail, Z.A. Ahmad, T. Ariga, L.B. Hussain, J. Teknologi 46(C) (June) (2007) 1–14.
[3] R. Mahmudi, A.R. Geranmayeh, H. Noori, M. Shahabi, Mater. Sci. Eng., A 491 (2008) 110–116.
[4] F. Ochoa, X. Deng, N. Chawla, J. Electron. Mater. 33 (12) (2004) 1596–1607.
[5] F. Ochoa, J.J Williams, N. Chawla, JOM (June) (2003) 56–60.
[6] H.U. Qiang, Z.S. Lee, Z.L. Zhao, D.L. Lee, International Conference on Asian Green Electronics, 2005, pp. 156–160.
[7] J.G. Maveety, P. Liu, J. Vijayen, F. Hua, E.A. Sanchez, J. Electron. Mater. 33 (11) (2004).
[8] F. Ochoa, J.J. Williams, N. Chawla, J. Electron. Mater. 32 (12) (2003) 1414–1420.
[9] R. Mahmudi, A.R. Geranmayeh, H. Noori, N. Jahangiri, H. Khanbareh, Mater. Sci. Eng., A 487 (2008) 20–25.
[10] S.K. Seo, S.K. Kang, D.Y. Shih, H.M. Lee, J. Electron. Mater. 38 (2) (2009).
[11] R. Peter, L. Tony, V. Bart, V. Bert, T. Steven, EMPC, June 12–15, Brugge, Belgium, 2005.
[12] P. Ratchev, B. Vandevelde, B. Verlinden, http://www.imec.be/ALSHIRA/ratchevbrussel.pdf (accessed on 14-7-2011).
[13] Y.S. Kim, K.S. Kim, C.W. Hwang, K. Suganuma, J. Alloys Compd. 352 (2003) 237–245.
[14] W.X. Chen, S. Xue, H. Wang, H. Yuhua, J. Wang, J. Mater. Sci: Mater. Electron. 21 (2010) 719–725.